

ALMA MATER STUDIORUM · UNIVERSITÀ DI BOLOGNA

Scuola di Scienze
Dipartimento di Fisica e Astronomia
Corso di Laurea in Fisica

Determination of CKM phases γ and $-2\beta_s$ from charmless two-body decays of beauty mesons

Relatore:

Prof./Dott. Angelo Carbone

Presentata da:

Davide Fasolo

Correlatore: (eventuale)

Prof./Dott. Stefano Perazzini

Year 2017/2018

Abstract An important task of the modern research in particle physics is to measure the properties of the Cabibbo-Kobayashi-Maskawa (CKM) matrix. The CKM matrix governs the mixing between mass and flavour eigenstates of quarks and is responsible of the breaking of the CP symmetry in the Standard Model (SM), hence, in the very end, of the imbalance between matter and anti-matter in the Universe. Probing the consistency and the unitarity of the CKM matrix is fundamental to verify the validity of the SM and to look for physics beyond. Using the measurements of CP-violation parameters and branching ratios of the $B^0 \rightarrow \pi^+ \pi^-$, $B^0 \rightarrow \pi^0 \pi^0$, $B^+ \rightarrow \pi^+ \pi^0$ and $B_s^0 \rightarrow K^+ K^-$ decays, a bayesian analysis is performed to determine two parameters of the CKM matrix: the angle γ and the mixing phase, $-2\beta_s$, of the B_s^0 meson.

Contents

1 Standard Model	5
1.1 Introduction to the Standard Model	5
1.2 The Feynman diagrams	7
1.3 The CKM matrix	8
1.4 Wolfenstein parameterization of the CKM matrix and unitary triangles	12
2 Hadronic two-body B decays	15
2.1 Direct CP asymmetries	16
2.2 Mixing of neutral B mesons	17
3 Bayesian analysis	21
3.1 Bayes theorem	21
3.2 Parametric inference	22
4 Measurement of the CKM parameters γ and $-2\beta_s$ using $B \rightarrow h^+h^-$ decays	25
4.1 Decay amplitudes	26
4.2 Determination of γ and $-2\beta_s$ from $B^0 \rightarrow \pi^+\pi^-$ and $B_s^0 \rightarrow K^+K^-$ decays	28
4.3 Inclusion of $B^0 \rightarrow \pi^0\pi^0$ and $B^+ \rightarrow \pi^+\pi^0$	35
5 Conclusions	39

Introduction

The study of the Cabibbo-Kobayashi-Maskawa (CKM) matrix is directly related to the flavour dynamics of quarks, and governs CP violation in the Standard Model (SM). Relevant tests of the role of the CKM matrix in the SM can be obtained by studying CP violation in some processes involving weak decays of B mesons. In a brief introduction of the SM we show that the CKM is a unitary complex matrix that can be parameterised by four parameters, three real angles and one complex phase. Testing the unitarity of the CKM matrix is one of the most powerful tools to probe the SM and to search for physics beyond it. This thesis focuses on the determination of two parameters of the CKM matrix: γ and $-2\beta_s$. These parameters can be determined with great accuracy from decays dominated by tree-level transitions, hence in cases where only SM contributions are expected. An alternative strategy is to determine them using decays receiving significant contributions from loop topologies, like two-body hadronic decays of B mesons ($B^0 \rightarrow \pi^+ \pi^-$, $B^0 \rightarrow \pi^0 \pi^0$, $B^+ \rightarrow \pi^+ \pi^0$ and $B_s^0 \rightarrow K^+ K^-$). The advantage of using these decays is that in the loops new particles, not present in the SM, may appear as virtual contributions modifying the values of the CP asymmetries and branching fractions with respect to their SM value. Hence, any deviation of γ and $-2\beta_s$ from their values determined from tree-level decays would be a proof of physics beyond the SM. Unfortunately the loop topologies introduce additional hadronic parameters in the decay amplitudes, that are a dangerous source of systematic uncertainties. However, several strategies have been proposed to minimize these effects and have already been tested. In this thesis we perform the same analyses, but updating the input measurements to the latest available results.

The thesis is organized as follow: a first chapter introduces the basic concepts of the SM, the Feynmann diagrams representing the interactions between particles, and the CKM matrix. In the second chapter a description of the hadronic two-body decays of B mesons is given, summarising the mechanism at the basis of CP violation in these decays. The third chapter is dedicated to the theory behind the bayesian analysis and how it can be applied in situation like the one at hand. In the fourth chapter we first present how the decay amplitudes of the used decays relate to the CKM parameters. Then, after summarising the measurements used as constraints in the analysis, the bayesian inference is used to determine γ and $-2\beta_s$. Particular attention is given in the analysis to the effect introduced by the theoretical assumptions used to deal with the hadronic parameters. In the final chapter the results of the analysis are summarised and briefly discussed.

Chapter 1

Standard Model

1.1 Introduction to the Standard Model

The Standard Model (SM) is a model used to describe the fundamental particles and antiparticles (which are particles having the same features of their own associated particles but opposite quantum numbers) and the nature of their interactions at high energy. This model divides the particles on many levels, but the two main types are defined by the nature of their spin. Particles with a semi-integer spin are called Fermions and are the fundamental constituents of matter, while particles with an integer spin are called Bosons and are responsible for the interactions.

Fermions are classified in two groups regarding whether or not they interact through strong interaction. Those that do are called Quarks, while the others are called Leptons. Both Leptons and Quarks can have electro-weak interactions. Both groups are composed of six different particles, organized in three "families", each one composed by a couple of particles. This scheme is symmetrically reproduced for the antiparticles.

The families of the Leptons have flavour of electron (L_e), muon (L_μ) and tau (L_τ). Each family is composed of a charged lepton (which gives the name to its family) and a characteristic neutrino with zero electrical charge.

$$\begin{pmatrix} \nu_e \\ e^- \end{pmatrix} \begin{pmatrix} \nu_\mu \\ \mu^- \end{pmatrix} \begin{pmatrix} \nu_\tau \\ \tau^- \end{pmatrix}. \quad (1.1)$$

Quark families are organized this way:

$$\begin{pmatrix} u \\ d \end{pmatrix} \begin{pmatrix} c \\ s \end{pmatrix} \begin{pmatrix} t \\ b \end{pmatrix}, \quad (1.2)$$

where the quark up (u), charm (c) and top (t) have an electrical charge $q_{up} = +\frac{2}{3}$ and the quark down (d), strange (s) and beauty (also called bottom) (b) have electrical charge $q_{down} = -\frac{1}{3}$, in units of the fundamental electric charge e . Every quark has a baryonic number of $\frac{1}{3}$. In addition a quantum number called flavour is assigned to each quark. This quantum number is

- strangeness $S = -1$ for the s quark,

- charmness $C = 1$ for the c quark,
- beautyness $B = -1$ for the b quark,
- topness $T = +1$ for the t quark.

Quarks are bound by the strong interaction to form hadrons. When three quarks are bound together they form a baryon with baryonic number 1, while when a quark (q) and an antiquark (\bar{q}) are bound together they form a meson with baryonic number 0. The quantum chromo dynamic (QCD), the theory that describes strong interactions, states that quarks can combine as long as their baryonic number is an integer, condition followed by both adrons and mesons.

Bosons are the mediators of the interactions. They are also called gauge bosons, because they follow from the gauge symmetry. These particles are the photon (γ), mediator of the electromagnetic interaction, the gluons (g), mediators of the strong interactions, the bosons W^\pm and Z^0 , mediators of the weak interactions, and the Higgs boson, which couples with the particles assigning them their mass.

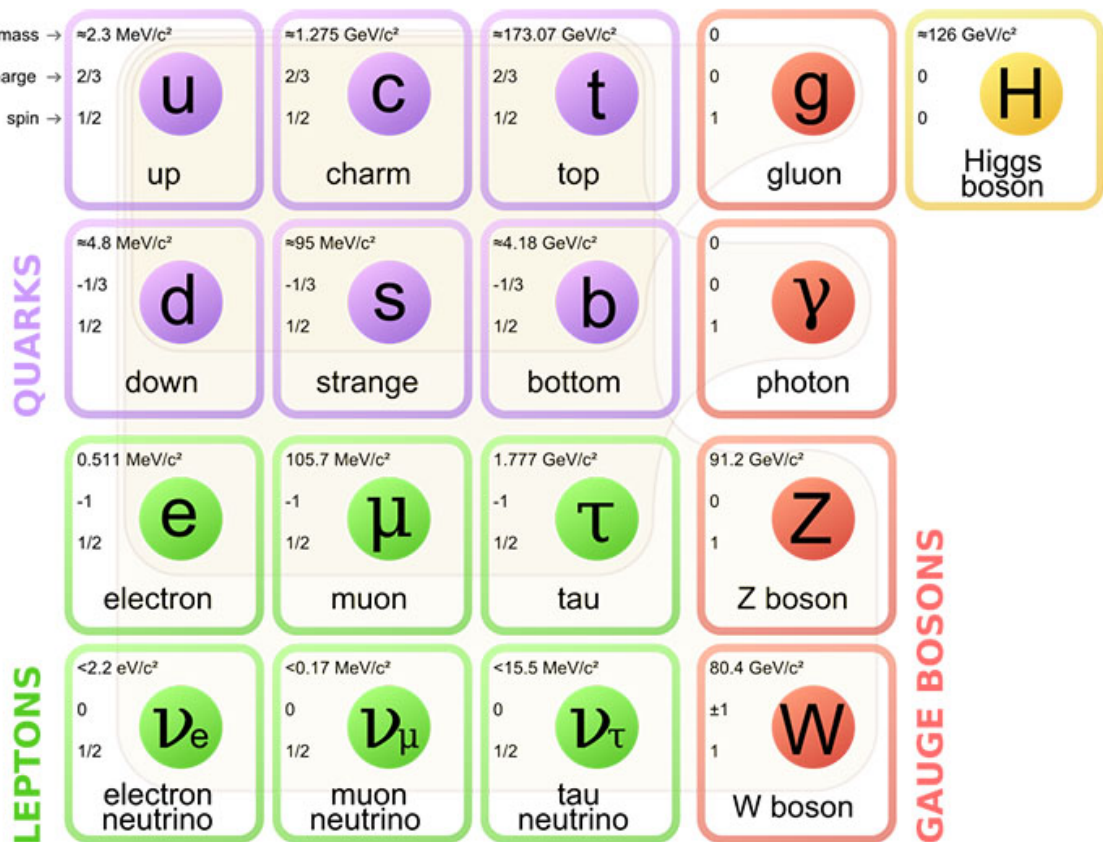


Figure 1.1: Scheme of the particle of the standard model, organized by families and nature.

1.2 The Feynman diagrams

A fairly simple but extremely functional way to describe interactions among particles is given by the so-called Feynman diagrams. These diagrams represent the particles and their interactions on a space-time frame, representing in different ways the various kinds of interaction involved.

As examples, in Figure 1.2 we can see the interaction of two electrons represented in a Feynman diagram, in Figure 1.3 we can see the annihilation of a quark and its corresponding antiquark resulting in the emission of a gluon and eventually in the creation of a top and antitop quark. Two examples Feynman diagrams for weak-interaction processes are reported in Figures 1.4 and 1.5. One thing to note is how

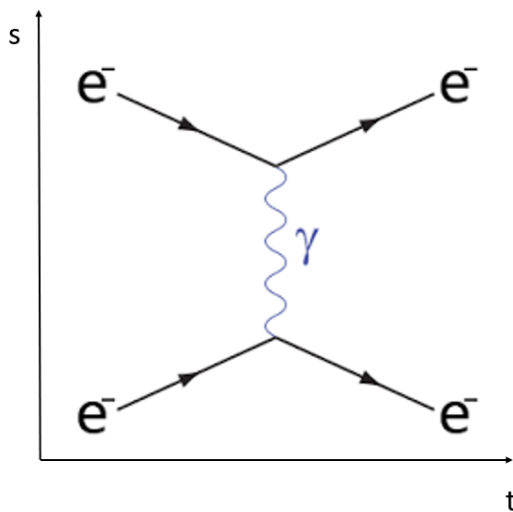


Figure 1.2: Feynman diagram of the electromagnetic repulsion between two e^- .

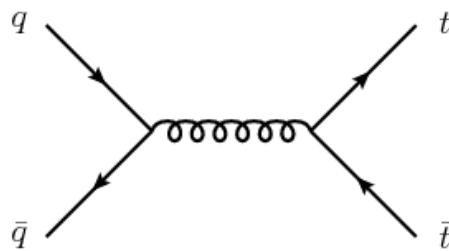


Figure 1.3: Feynman diagram of the strong annihilation of a generic quark and antiquark with the emission of a gluon and the generation of a couple top-antitop.

this representation shows really well the concept of the interactions being mediated by bosons, picturing them as mediators between the initial and final particles. It should be noted that each vertex of the diagram is associated to a coupling constant, which represents the strength of the interaction.

1.3 The CKM matrix

As seen in the previous section, the probability for a process to occur is proportional to the coupling constant of the vertex in the Feynman diagram. For the strong and electromagnetic interactions the coupling constant is independent of the family of particles. In the case of weak interaction, however, this is not the case. In fact there are experimental evidences that the strength of weak interaction depends on the flavour of the involved particles. This phenomenon has been explained by Cabibbo in 1963 [1]. At that time only the u, d and s quarks were known and experimental observations evidenced that in hadronic decays,

- some decays have variation of strangeness $|\Delta S| = 0$ while others shows $|\Delta S| = 1$,
- processes with strangeness variation $|\Delta S| = 0$ are preferred over those with $|\Delta S| = 1$.

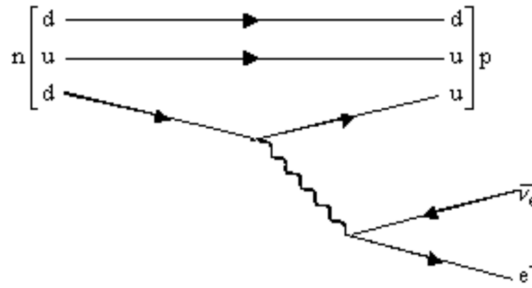


Figure 1.4: Feynman diagram of the β decay. A conversion of a quark d in a quark u with the emission of a W^- boson, which later generates a couple e^- and ν_e .

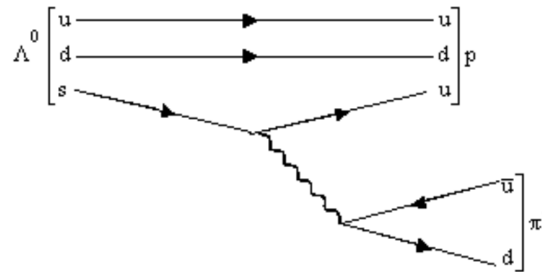


Figure 1.5: Feynman diagram of the Λ^0 decay. A conversion of a quark s in a quark u with the emission of a W^- boson, which later generates a couple \bar{u} and d .

Considering for example the two decays:

$$n \rightarrow p e^- \bar{\nu}_e \quad (1.3a)$$

$$\Lambda \rightarrow p \pi^- \quad (1.3b)$$

We can see that the quark composition of the hadrons involved are:

$$\begin{aligned}
 n &= \begin{pmatrix} u \\ d \\ d \end{pmatrix}, \quad S = 0 \\
 p &= \begin{pmatrix} u \\ u \\ d \end{pmatrix}, \quad S = 0 \\
 \Lambda &= \begin{pmatrix} s \\ d \\ u \end{pmatrix}, \quad S = -1 \\
 \pi^- &= \begin{pmatrix} \bar{u} \\ d \end{pmatrix}, \quad S = 0.
 \end{aligned} \tag{1.4}$$

We can see that in the decay of Eq. (1.3a) we have $|\Delta S| = 0$ while in the one of Eq. (1.3b) $|\Delta S| = 1$.

In his paper Cabibbo proposed to consider the down-type (d and s) quarks in the interactions not as pure flavour eigenstates, but instead as linear combinations d' and s' , such that both $(d \ s)$ and $(d' \ s')$ pairs constitute an orthonormal basis for the description of the quark state involved in the transition. The eigenstates d' and s' correspond to a rotation by the so-called Cabibbo angle of the flavour eigenstates d and s:

$$\begin{pmatrix} d' \\ s' \end{pmatrix} = \begin{pmatrix} V_{ud} & V_{us} \\ V_{cd} & V_{cs} \end{pmatrix} \begin{pmatrix} d \\ s \end{pmatrix} = \begin{pmatrix} \cos \theta_C & \sin \theta_C \\ -\sin \theta_C & \cos \theta_C \end{pmatrix} \begin{pmatrix} d \\ s \end{pmatrix} \tag{1.5}$$

In this way it was possible to explain the suppression of $\Delta S = 0$ processes. In fact,

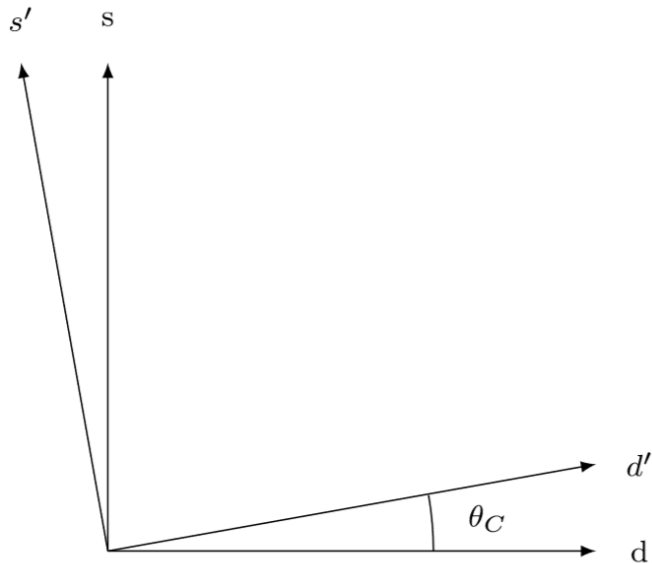


Figure 1.6: Rotation of a θ_C angle of the (d s).

since the weak interaction acts on flavour eigenstates, the couplings of the decays in Eqs. (1.3a) and (1.3b) are hence proportional to $\cos \theta_C$ and $\sin \theta_C$ respectively. The

Cabibbo angle is observed to be small, so that the interaction which preserve the strangeness is easier to find than the other.

The generalization of the Cabibbo idea with all the three families of quarks was then proposed by M. Kobayashi and K. Maskawa [1, 2]. The matrix of Eq. (1.5) was replaced with the Cabibbo-Kobayashi-Maskawa (CKM) matrix V :

$$\begin{pmatrix} d' \\ s' \\ b' \end{pmatrix} = \begin{pmatrix} V_{ud} & V_{us} & V_{ub} \\ V_{cd} & V_{cs} & V_{cb} \\ V_{td} & V_{ts} & V_{tb} \end{pmatrix} \begin{pmatrix} d \\ s \\ b \end{pmatrix} = V \begin{pmatrix} d \\ s \\ b \end{pmatrix}, \quad (1.6)$$

that is a complex unitary matrix, hence respects the condition:

$$V^\dagger V = 1 = VV^\dagger. \quad (1.7)$$

This relation of unitarity corresponds to nine equations. Three of these equations express the universality of weak interaction:

$$|V_{ud}|^2 + |V_{us}|^2 + |V_{ub}|^2 = 1, \quad (1.8a)$$

$$|V_{cd}|^2 + |V_{cs}|^2 + |V_{cb}|^2 = 1, \quad (1.8b)$$

$$|V_{td}|^2 + |V_{ts}|^2 + |V_{tb}|^2 = 1, \quad (1.8c)$$

while the other six equations define the orthogonality relations and can be represented as triangles in a complex plane:

$$V_{ud}^* V_{us} + V_{cd}^* V_{cs} + V_{td}^* V_{ts} = 0, \quad (1.9a)$$

$$V_{ub}^* V_{ud} + V_{cb}^* V_{cd} + V_{tb}^* V_{td} = 0, \quad (1.9b)$$

$$V_{us}^* V_{ub} + V_{cs}^* V_{cb} + V_{ts}^* V_{tb} = 0, \quad (1.9c)$$

$$V_{cd} V_{ud}^* + V_{cs} V_{us}^* + V_{cb} V_{ub}^* = 0, \quad (1.9d)$$

$$V_{td} V_{ud}^* + V_{ts} V_{us}^* + V_{tb} V_{ub}^* = 0, \quad (1.9e)$$

$$V_{td} V_{cd}^* + V_{ts} V_{cs}^* + V_{tb} V_{cb}^* = 0, \quad (1.9f)$$

The requirements of Eqs. (1.8) and (1.9) reduce the number of free parameters of the CKM matrix to four: three real mixing angles and one complex phase. This complex phase, is responsible for the CP violation in the SM.

Using a 3-dimensional space (d, s, b) we can obtain the real part of the mixing matrix using some transformations. In particular we are interested in the case where this is accomplished with three rotations: first we rotate around the b-axis of an angle θ_{12} , then around the s axis of an angle θ_{13} and finally around the d axis of an angle θ_{23} . Defining $c_{ij} = \cos \theta_{ij}$ and $s_{ij} = \sin \theta_{ij}$ the real CKM matrix calculated this way looks like:

$$Re|V| = \begin{pmatrix} 1 & 0 & 0 \\ 0 & c_{23} & s_{23} \\ 0 & -s_{23} & c_{23} \end{pmatrix} \begin{pmatrix} c_{13} & 0 & s_{13} \\ 0 & 1 & 0 \\ -s_{13} & 0 & c_{13} \end{pmatrix} \begin{pmatrix} c_{12} & -s_{12} & 0 \\ s_{12} & c_{12} & 0 \\ 0 & 0 & 1 \end{pmatrix} \quad (1.10)$$

The values of the angles are measured to be [4]

$$\theta_{12} = (12.78 \pm 0.06)^\circ \quad (1.11a)$$

$$\theta_{23} = (2.41 \pm 0.03)^\circ \quad (1.11b)$$

$$\theta_{13} = (0.211 \pm 0.005)^\circ \quad (1.11c)$$

From this matrix we can obtain V adding the complex phase δ_{13} in the calculus:

$$\begin{aligned} V &= \begin{pmatrix} 1 & 0 & 0 \\ 0 & c_{23} & s_{23} \\ 0 & -s_{23} & c_{23} \end{pmatrix} \begin{pmatrix} c_{13} & 0 & s_{13}e^{-i\delta_{13}} \\ 0 & 1 & 0 \\ -s_{13}e^{+i\delta_{13}} & 0 & c_{13} \end{pmatrix} \begin{pmatrix} c_{12} & -s_{12} & 0 \\ s_{12} & c_{12} & 0 \\ 0 & 0 & 1 \end{pmatrix} \quad (1.12) \\ &= \begin{pmatrix} c_{12}c_{13} & s_{12}c_{13} & s_{13}e^{-i\delta_{13}} \\ s_{12}c_{23} - c_{12}s_{23}s_{13}e^{+i\delta_{13}} & c_{12}c_{13} - s_{12}s_{23}s_{13}e^{+i\delta_{13}} & s_{23}c_{13} \\ s_{12}s_{23} - c_{12}c_{23}s_{13}e^{+i\delta_{13}} & c_{12}s_{23} - s_{12}c_{23}s_{13}e^{+i\delta_{13}} & c_{23}c_{13} \end{pmatrix} \end{aligned}$$

All the θ_{ij} angles can be chosen to lie in the first quadrant and the mixing between two quarks generation i,j vanishes if the corresponding θ_{ij} is equal to zero.

In particular, in the case $\theta_{13} = \theta_{23} = 0$ the CKM matrix would take the form of the V_C from Eq (1.5).

The values of the CKM matrix elements have been measured by studying the following processes:

- $|V_{ud}| \rightarrow$ Nuclear beta decays ($d \rightarrow ue\nu_e$ transitions)
- $|V_{us}| \rightarrow$ Semileptonic kaons decays $K \rightarrow \pi l\bar{\nu}$ ($s \rightarrow ul\bar{\nu}$ transitions)
- $|V_{ub}| \rightarrow$ Exclusive and inclusive semileptonic B-hadron decays ($b \rightarrow ul\bar{\nu}$ transitions)
- $|V_{cd}| \rightarrow$ Semileptonic D-hadron decays $D \rightarrow \pi l\bar{\nu}$ ($c \rightarrow dl\bar{\nu}$ transitions) and charm production from ν interaction with matter
- $|V_{cs}| \rightarrow$ Semileptonic D decays ($c \rightarrow sl\bar{\nu}$ transitions) and leptonic D_s decays ($D_s \rightarrow l\bar{\nu}$)
- $|V_{cb}| \rightarrow$ Exclusive and inclusive semileptonic B decays to charm ($b \rightarrow cl\nu$ transitions)
- $|V_{tb}| \rightarrow$ Branching fraction of $t \rightarrow Wb$ decay (assuming CKM matrix unitarity) and single top-quark-production cross section.

The magnitudes of V_{td} and V_{ts} are not measurable using tree-level processes. The cleanest way to measure them is to determine $\frac{V_{td}}{V_{ts}}$ from $B^0 - \bar{B}^0$ and $B_s^0 - \bar{B}_s^0$ oscillation processes.

The magnitudes of the elements of the CKM matrix are [3]:

$$V = \begin{pmatrix} |V_{ud}| & |V_{us}| & |V_{ub}| \\ |V_{cd}| & |V_{cs}| & |V_{cb}| \\ |V_{td}| & |V_{ts}| & |V_{tb}| \end{pmatrix} = \begin{pmatrix} 974.20 \pm 0.21 & 224.3 \pm 0.5 & 3.94 \pm 0.36 \\ 218 \pm 4 & 997 \pm 17 & 42.2 \pm 0.8 \\ 8.1 \pm 0.5 & 39.4 \pm 2.3 & 1019 \pm 25 \end{pmatrix} \times 10^{-3}. \quad (1.13)$$

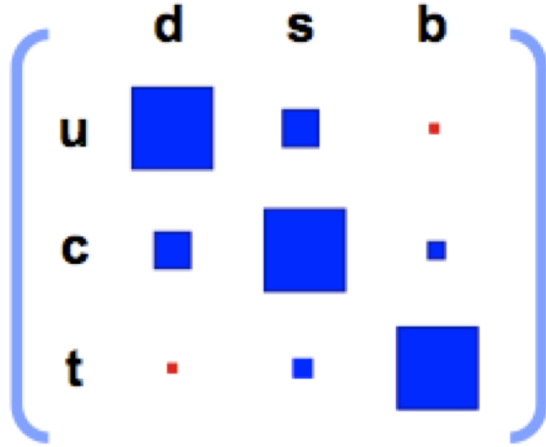


Figure 1.7: Graphic representation of the magnitudes of the CKM matrix elements and of their hierarchies

The squared values of these modules are proportional to the transition rates of processes between a down-like quark ($d \ s \ b$) and an up-like one ($u \ c \ t$).

Analyzing the values in Eq. (1.13) we can see that the terms on the diagonal are definitely bigger than the others, showing the already known fact that transitions between quark of the same family are strongly favorite. We can also see that transitions between the first and second generation are more probable than the ones between the second and the third generation. The least probable transitions are those involving the first and the third generation, meaning that the decays are more likely to happen between generations next to each other.

1.4 Wolfenstein parameterization of the CKM matrix and unitary triangles

Considering the hierarchy of the elements of the CKM matrix, L. Wolfenstein proposed a parameterization of the matrix in terms of powers of $\sin \theta_C$ [18]. By substituting in Eq. (1.10) the terms:

$$s_{12} = \lambda \quad (1.14a)$$

$$s_{23} = A\lambda^2 \quad (1.14b)$$

$$s_{13}e^{-i\delta_{13}} = A\lambda^3(\rho - i\eta), \quad (1.14c)$$

the CKM matrix can be written as:

$$V = \begin{pmatrix} 1 - \frac{\lambda^2}{2} & \lambda & A\lambda^3(\rho - i\eta) \\ \lambda & 1 - \frac{\lambda^2}{2} & A\lambda^2 \\ A\lambda^3(1 - \rho - i\eta) & -A\lambda^2 & 1 \end{pmatrix} + O(\lambda^4) \quad (1.15)$$

Considering Eq. (1.7), and interpreting the sides of the triangles in terms of power of λ , we can see that the triangles that are not squashed are those defined in Eqs. (1.9b)

and (1.9e), which have all sides of the same order of magnitude.

It is convenient for our analysis to rewrite the triangles so that one side is unitary.

$$\frac{V_{ub}^* V_{ud}}{V_{cb}^* V_{cd}} + 1 + \frac{V_{tb}^* V_{td}}{V_{cb}^* V_{cd}} = 0 \quad (1.16a)$$

$$\frac{V_{td} V_{ud}^*}{V_{ts} V_{us}^*} + 1 + \frac{V_{tb} V_{ub}^*}{V_{ts} V_{us}^*} = 0 \quad (1.16b)$$

We concentrate our study on the first triangle, which is particularly interesting for

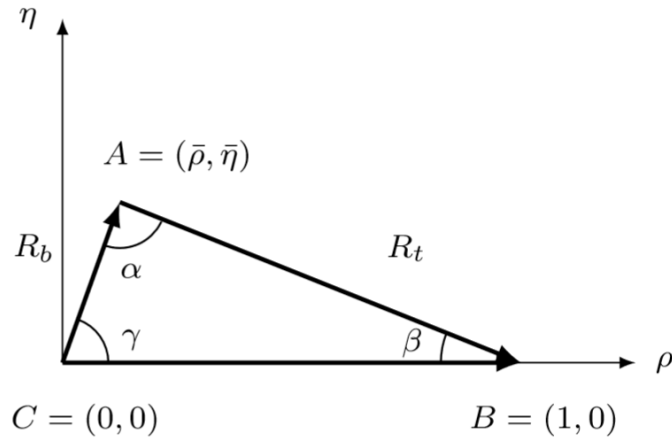


Figure 1.8: Triangle representing the unitary condition of Eq. (1.16a)

our case. Applying the Wolfenstein parameterization we can write:

$$\begin{cases} \frac{V_{ub}^* V_{ud}}{V_{cb}^* V_{cd}} = \frac{A\lambda^3(1-\frac{\lambda^2}{2})(\rho+i\eta)}{-A\lambda^3} = \frac{A\lambda^3(\rho+i\eta)}{-A\lambda^3} + O(\lambda^4) \\ \frac{V_{tb}^* V_{td}}{V_{cb}^* V_{cd}} = \frac{A\lambda^3(1-\rho-i\eta)}{-A\lambda^3} + O(\lambda^4) \end{cases} \quad (1.17)$$

We can define the generalized parameters:

$$\bar{\rho} = (1 - \frac{\lambda^2}{2})\rho \quad \bar{\eta} = (1 - \frac{\lambda^2}{2})\eta \quad (1.18)$$

The equation for the unitary triangle is calculated as:

$$(1 - \bar{\rho} - i\bar{\eta}) + (-1) + (\bar{\rho} + i\bar{\eta}) = 0 \quad (1.19)$$

The modules of the vectors in the new parameterization are:

$$\begin{cases} \bar{AC} = \frac{|V_{ub}^* V_{ud}|}{|V_{cb}^* V_{cd}|} = |(\bar{\rho} + i\bar{\eta})|^2 = R_b \\ \bar{BC} = 1 \\ \bar{AB} = \frac{|V_{tb}^* V_{td}|}{|V_{cb}^* V_{cd}|} = |(1 - \bar{\rho} - i\bar{\eta})|^2 = R_t \end{cases} \quad (1.20)$$

These equations in a complex plane $(\rho \quad \eta)$ represent the unitary triangle as shown in Figure 1.8.

The values of the angles inside the triangle are then given by:

$$\alpha = \arg \left(\frac{V_{ub}^* V_{ud}}{V_{tb}^* V_{td}} \right) \quad (1.21a)$$

$$\beta = \arg \left(\frac{V_{tb}^* V_{td}}{V_{cb}^* V_{cd}} \right) = \arctan \frac{\bar{\eta}}{1 - \bar{\rho}} \quad (1.21b)$$

$$\gamma = \arg \left(\frac{V_{ub}^* V_{ud}}{V_{cb}^* V_{cd}} \right) = \arctan \frac{\bar{\eta}}{\bar{\rho}} \quad (1.21c)$$

The other triangle defined in Eq. (1.16b) is the same as the one in Eq. (1.16a) but rotated by the angle β_s corresponding to

$$\beta_s = \arg \left(-\frac{V_{ts} V_{tb}^*}{V_{cs} V_{cb}^*} \right). \quad (1.22)$$

The experimental determination of the sides R_t and R_b and of the angles α , β , γ and β_s is fundamental to verify the validity of the SM. The determination of these parameters can be obtained from the study of many different decays. If the various measurements should not agree with a common apex of the UT, it would mean that the CKM model of CP violation is incomplete and requires more particles that are currently not present in the SM.

Chapter 2

Hadronic two-body B decays

The B meson is a meson composed by a quark and an antiquark of the form $(q \bar{q})$. Of particular interest for this thesis is the case where $q \in \{d, s\}$ generating the neutral mesons B^0 and B_s^0 respectively.

Hadronic two-body B meson decays are fairly important for the exploration of the CP violation. The Feynman diagrams describing the topologies contributing to the amplitudes of these decays can be divided in two groups: tree-level diagrams and loop diagrams(also referred to as penguin diagrams). An example of these diagrams is reported in Figure 2.1.

Each vertex of a Feynman diagrams contribute to the decay amplitude with a

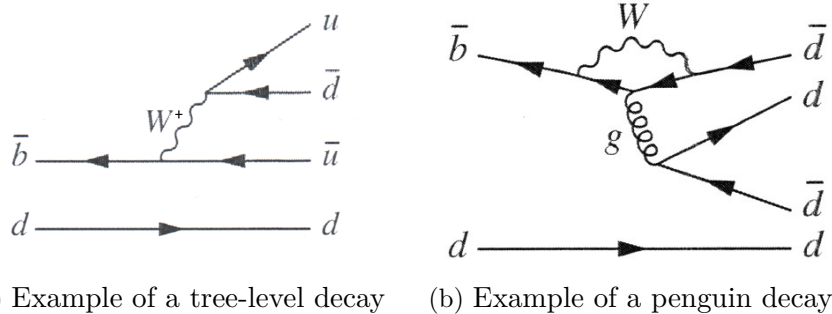


Figure 2.1: Examples of a tree-level decay (a): an antiquark \bar{b} becomes an antiquark \bar{u} , emitting a W^+ boson, which then generates a meson π^+ , $(u \bar{d})$, and of a penguin decay (b) with emission of a g boson, which generates a π^0 meson

complex term. This term takes into account the strength and the phase due to the interaction and the CKM elements corresponding to the quark-level transitions. An important thing to note is that under CP transformation only the phase of CKM elements change sign, while the other phase of the amplitude does not. For example in the diagram in Figure 2.1 the decay amplitude will be proportional to the CKM elements

$$A \propto V_{ub}^* V_{ud}, \quad (2.1a)$$

$$A \propto V_{tb}^* V_{td}, \quad (2.1b)$$

for the left and right diagrams, respectively. Another process governing neutral B meson decays is the so-called $B_q^0 - \bar{B}_q^0$ mixing. This process is the oscillation of a neutral B_q^0 meson into its antiparticle and is governed by the Feynman diagrams in Figure 2.2.

In this case we see that the CKM elements involved are $V_{qd(s)}$ and V_{qb}^* , where the case in which q is the t quark is the dominant one.

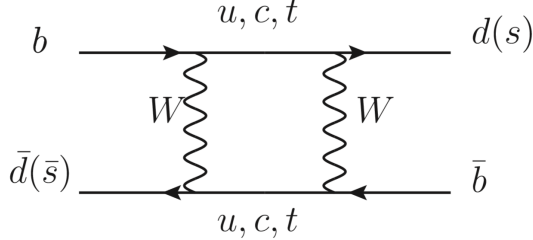


Figure 2.2: Example of $B_q^0 - \bar{B}_q^0$ mixing

2.1 Direct CP asymmetries

Considering a decay governed by the diagrams in Figure 2.1, the amplitude of the decay can be written as:

$$A = A_1 e^{i\delta_1} e^{i\phi_1} + A_2 e^{i\delta_2} e^{i\phi_2} \quad (2.2)$$

Where A_1 and A_2 are the modules of the amplitude of the two diagrams, δ_1 and δ_2 are the so-called strong phases and ϕ_1 and ϕ_2 are derived from the CKM elements. The amplitude of the CP-conjugated decay can be written as:

$$\bar{A} = A_1 e^{i\delta_1} e^{-i\phi_1} + A_2 e^{i\delta_2} e^{-i\phi_2}. \quad (2.3)$$

The modules squared of the amplitudes in Eqs. (2.1) and (2.2) represent the probability of the transition of a generic B meson to the final state f and the CP-conjugated process, respectively.

The asymmetry between these probabilities can be written as:

$$\begin{aligned} A_{CP} &\equiv \frac{\Gamma(\bar{B} \rightarrow \bar{f}) - \Gamma(B \rightarrow f)}{\Gamma(\bar{B} \rightarrow \bar{f}) + \Gamma(B \rightarrow f)} = \frac{|A(\bar{B} \rightarrow \bar{f})|^2 - |A(B \rightarrow f)|^2}{|A(\bar{B} \rightarrow \bar{f})|^2 + |A(B \rightarrow f)|^2} = \\ &= \frac{2|A_1||A_2|\sin(\delta_1 - \delta_2)\sin(\phi_1 - \phi_2)}{|A_1|^2 + 2|A_1||A_2|\cos(\delta_1 - \delta_2)\cos(\phi_1 - \phi_2) + |A_2|^2}. \end{aligned} \quad (2.4)$$

A non vanishing CP asymmetry A_{CP} indicates that the behaviour of the particle B is different from the behaviour of its antiparticle \bar{B} . CP violation arises from the interference between the two amplitudes corresponding to the two diagrams in Figure 2.1. This is referred to as direct CP violation.

Since the weak phase difference is generally given by one of the angles of the unitary triangles, it is possible to determine this angle from the measured value of A_{CP} . However, the extraction of $(\phi_1 - \phi_2)$ from A_{CP} is problematic because the number

of unknowns includes also the amplitudes $|A_{1,2}|$ and the strong phase difference $(\delta_1 - \delta_2)$. It is possible to deal with this problem, searching for fortunate cases, where relations between decay amplitudes of different channels allow to use more CP-violation observables and to overconstraint the system of equations determining also the values of the hadronic parameters.

2.2 Mixing of neutral B mesons

Another source of CP violation in neutral B meson decays is the CP violation arising from the interference between $B_q^0 - \bar{B}_q^0$ mixing and decay processes. This is called the mixing-induced CP violation.

2.2.1 Neutral mixing

The phenomenon of neutral mixing arises from the box-diagrams shown in Figure 2.2. At any time t the B meson can be seen as a superposition of states:

$$|B(t)\rangle = a(t)|B\rangle + b(t)|\bar{B}\rangle, \quad (2.5)$$

where $|B\rangle$ and $|\bar{B}\rangle$ represent the particle and antiparticle state of the B_q^0 meson, $a(t)$ and $b(t)$ are the coefficients of each state as a function of time and satisfy the relation:

$$|a(t)|^2 + |b(t)|^2 = 1. \quad (2.6)$$

The time evolution is thus governed by a 2×2 effective hamiltonian, which can be expressed in terms of the Hermitian matrices M and Γ :

$$H = M - \frac{i}{2}\Gamma = \begin{pmatrix} M & M_{12} \\ M_{12}^* & M \end{pmatrix} - \frac{i}{2} \begin{pmatrix} \Gamma & \Gamma_{12} \\ \Gamma_{12}^* & \Gamma \end{pmatrix}. \quad (2.7)$$

The elements of this matrix are related to the amplitudes of the vertices in the Feynman diagrams in Figure 2.2. The matrix diagonal elements have to be equal to guarantee the invariance of the system for CPT transformations.

The time evolution of a neutral B meson can hence be described by a Schrödinger equation of the form:

$$i\frac{d}{dt} \begin{pmatrix} a(t) \\ b(t) \end{pmatrix} = H \begin{pmatrix} a(t) \\ b(t) \end{pmatrix}. \quad (2.8)$$

Solving for the eigenvalue of H we obtain two eigenstates of masses $M_{H,L}$ and widths $\Gamma_{H,L}$, respectively :

$$|B_H\rangle = \frac{p|B\rangle + q|\bar{B}\rangle}{\sqrt{|p|^2 + |q|^2}}, \quad (2.9a)$$

$$|B_L\rangle = \frac{p|B\rangle - q|\bar{B}\rangle}{\sqrt{|p|^2 + |q|^2}}, \quad (2.9b)$$

corresponding to the eigenvalues:

$$\lambda_H = M - \frac{i}{2}\Gamma + \frac{q}{p}(M_{12} - \frac{i}{2}\Gamma_{12}), \quad (2.10a)$$

$$\lambda_L = M - \frac{i}{2}\Gamma - \frac{q}{p}(M_{12} - \frac{i}{2}\Gamma_{12}), \quad (2.10b)$$

where we have defined:

$$\frac{q}{p} = \sqrt{\frac{M_{12}^* - \frac{i}{2}\Gamma_{12}^*}{M_{12} - \frac{i}{2}\Gamma_{12}}}. \quad (2.11)$$

Note that each mass eigenstate $|B_H\rangle$ and $|B_L\rangle$ can be expressed as a linear combination of the flavour eigenstates $|B\rangle$ and $|\bar{B}\rangle$. The time evolution of a pure B meson generated in the pure $|B\rangle$ state, hence having $b(0) = 0$, is:

$$|B(t)\rangle = g_+(t)|B\rangle + \frac{q}{p}g_-(t)|\bar{B}\rangle. \quad (2.12)$$

The opposite case of a B meson generated in the pure $|\bar{B}\rangle$ state is instead:

$$|\bar{B}(t)\rangle = g_+(t)|\bar{B}\rangle + \frac{p}{q}g_-(t)|B\rangle, \quad (2.13)$$

where the time-dependent coefficients $g_+(t)$ and $g_-(t)$ are:

$$g_+(t) = \left(\frac{e^{-i\lambda_H t} + e^{-i\lambda_L t}}{2} \right), \quad (2.14a)$$

$$g_-(t) = \left(\frac{e^{-i\lambda_H t} - e^{-i\lambda_L t}}{2} \right). \quad (2.14b)$$

Considering now the decay $B \rightarrow f$, the time-dependent amplitudes dependent from the time of this process will be, for the two cases of Eqs. (2.12) and (2.13),

$$\langle f | H_{eff} | B(t) \rangle, \quad (2.15a)$$

$$\langle f | H_{eff} | \bar{B}(t) \rangle, \quad (2.15b)$$

that, if expanded, will be:

$$A_{B \rightarrow f}(t) = g_+(t)\langle f | H_{eff} | B \rangle + \frac{q}{p}g_-(t)\langle f | H_{eff} | \bar{B} \rangle, \quad (2.16a)$$

$$A_{\bar{B} \rightarrow f}(t) = g_+(t)\langle f | H_{eff} | \bar{B} \rangle + \frac{p}{q}g_-(t)\langle f | H_{eff} | B \rangle, \quad (2.16b)$$

where $\langle f | H_{eff} | B \rangle = A_f$ and $\langle f | H_{eff} | \bar{B} \rangle = \bar{A}_f$ are the instantaneous decay amplitudes of $B \rightarrow f$ and $\bar{B} \rightarrow f$. From the amplitudes above it is possible to determine the time dependent decay rates by computing the module squared of the amplitudes:

$$\Gamma_{B \rightarrow f}(t) \propto |A_{B \rightarrow f}(t)|^2 = |A_f|^2 |g_+(t) + \lambda_f g_-(t)|^2, \quad (2.17a)$$

$$\Gamma_{\bar{B} \rightarrow f}(t) \propto |A_{\bar{B} \rightarrow f}(t)|^2 = |A_f|^2 |\frac{p}{q}|^2 |g_+(t) + g_-(t)|^2, \quad (2.17b)$$

where

$$\lambda_f = \frac{q}{p} \frac{\bar{A}_f}{A_f} \quad (2.18)$$

is the parameter governing the mixing induced CP violation. A last useful transformation is to rewrite Eqs. (2.10a) and (2.10b) as:

$$\lambda_H = M + \frac{\Delta M}{2} - \frac{i}{2} \left(\Gamma + \frac{\Delta \Gamma}{2} \right), \quad (2.19a)$$

$$\lambda_L = M - \frac{\Delta M}{2} - \frac{i}{2} \left(\Gamma - \frac{\Delta \Gamma}{2} \right). \quad (2.19b)$$

With this transformation and expanding the modules squared of the time dependent decay rates we obtain:

$$\Gamma_{B \rightarrow f}(t) = |A_f|^2 (I_+(t) + I_-(t)), \quad (2.20a)$$

$$\Gamma_{\bar{B} \rightarrow f}(t) = l |A_f|^2 \left| \frac{p}{q} \right|^2 (I_+(t) - I_-(t)), \quad (2.20b)$$

where

$$I_+(t) = (1 + |\lambda_f|^2) \cosh \left(\frac{\Delta \Gamma}{2} t \right) - 2R(\lambda_f) \sinh \left(\frac{\Delta \Gamma}{2} t \right), \quad (2.21a)$$

$$I_-(t) = (1 - |\lambda_f|^2) \cos(\Delta M t) - 2I(\lambda_f) \sin(\Delta M t). \quad (2.21b)$$

2.2.2 CP violating parameters

The CP violating term λ_f can be separated in two components. The term $\frac{q}{p}$ arises from the CKM elements entering the feynman diagram in Figure 2.2. Instead the terms A_f and \bar{A}_f contain the CKM elements appearing in the Feynman diagrams in Figure 2.1. Using Eqs. (2.20) it is possible to write the time dependent CP asymmetry:

$$\begin{aligned} A_{CP}(t) &= \frac{\Gamma_{\bar{B} \rightarrow f}(t) - \Gamma_{B \rightarrow f}(t)}{\Gamma_{\bar{B} \rightarrow f}(t) + \Gamma_{B \rightarrow f}(t)} = \\ &= \frac{(|\lambda_f|^2 - 1) \cos(\Delta M t) + 2I(\lambda_f) \sin(\Delta M t)}{(|\lambda_f|^2 + 1) \cosh(\frac{\Delta \Gamma}{2} t) - 2R(\lambda_f) \sinh(\frac{\Delta \Gamma}{2} t)} = \\ &= \frac{-C_f \cos(\Delta M t) + S_f \sin(\Delta M t)}{\cosh(\frac{\Delta \Gamma}{2} t) - A_f^{\Delta \Gamma} \sinh(\frac{\Delta \Gamma}{2} t)} \end{aligned} \quad (2.22)$$

where:

$$C_f = \frac{1 - |\lambda_f|^2}{1 + |\lambda_f|^2}, \quad (2.23a)$$

$$S_f = \frac{2I(\lambda_f)}{|\lambda_f|^2 + 1}, \quad (2.23b)$$

$$A_f^{\Delta \Gamma} = \frac{2R(\lambda_f)}{|\lambda_f|^2 + 1}, \quad (2.23c)$$

and we assumed $\left| \frac{q}{p} \right| \simeq 1$, that is well supported by experimental results independent of those used in this thesis. The three Eqs. (2.23) satisfy the relation:

$$|C_f|^2 + |S_f|^2 + |A_f^{\Delta\Gamma}|^2 = 1. \quad (2.24)$$

In the case of $C_f \neq 0$ we can speak of CP violation in the decay process. The parameter S_f , instead, parameterises the CP violation due to the interference between mixing and decay.

Chapter 3

Bayesian analysis

In the bayesian statistic the hypothesis that a certain theoretical model, dependent on a set of fundamental parameters $\{\theta_i\}$, is true is assumed and then tested against some given data $\{d_i\}$. The final aim is to obtain the probability that a given set of values for the parameters $\{\theta_i\}$ would have produced the observed experimental results $\{d_i\}$. This probability is called posterior probability. Hence, the posterior probability represents the distribution of the parameters that one would get repeating multiple times the experiment. Finally, from the posterior distribution is possible to compute the credibility intervals for the various parameters governing the model.

3.1 Bayes theorem

Let's consider a complete group of incompatible hypotheses H_1, H_2, \dots, H_n and that the result A is obtained from an experiment. The probability of the validity of hypothesis H_k given the result A is:

$$P(H_k|A) = \frac{P(A|H_k)P(H_k)}{\sum_{i=1}^n P(H_i)P(A|H_i)} \quad (3.1)$$

demonstration

The multiplication rule of probability states:

$$P(AH_i) = P(A|H_i)P(H_i) = P(H_i|A)P(A). \quad (3.2)$$

Solving respect to $P(H_i|A)$ we obtain:

$$P(H_i|A) = \frac{P(A|H_i)P(H_i)}{P(A)}. \quad (3.3)$$

The probability that A is verified is the sum on the n hypotheses of the products $P(A|H_i) P(H_i)$:

$$P(A) = \sum_{i=1}^n P(H_i)P(A|H_i) \quad (3.4)$$

Finally, substituting Eq. (3.4) in (3.3) we obtain the equation of the Bayes theorem. The generalization to the continuum case of Eq (3.1) is:

$$P(H|A) = \frac{P(A|H)P(H)}{\int P(H)P(A|H)dH}, \quad (3.5)$$

where the terms of this equation are probability densities defined as follows:

- $P(A|H)$ is also called *likelihood*
- $P(H)$ is also called *prior probability*
- $P(H|A)$ is also called *posterior probability*

3.2 Parametric inference

It is called parametric inference the method that, given a model interpreting a set of data, makes a afterwards measurement of the unknown parameters of the model, using the bayesian statistic.

The Bayes theorem has a key role in the application of this method. Given a generic parameter θ and a variable d representing a measurable quantity, Eq eq:3.5 can be rewritten as:

$$P(\theta|d) = \frac{P(d|\theta)P(\theta)}{\int P(d|\theta)P(\theta)d\theta}, \quad (3.6)$$

where $P(\theta)$ is the prior probability, $P(\theta|d)$ the posterior probability and $P(d|\theta)$ the likelihood. The denominator is a renormalization factor and is also called “evidence”. Posterior probability distributions describe our knowledge of the parameters and are used to calculate the confidence intervals, which are the probability that the true value of a given parameter lies in a certain interval.

A typical example for the likelihood is the Gaussian function. Suppose to measure the quantity d with error σ and that d is the direct measurement of the parameter μ of a theoretical model. The likelihood for μ to be responsible of the observation d is:

$$P(d|\mu, \sigma) = \frac{1}{\sqrt{2\pi}\sigma} e^{-\frac{(d-\mu)^2}{2\sigma^2}} \quad (3.7)$$

Substituting this likelihood in Eq. (3.6) we obtain:

$$P(\mu|d, \sigma) = \frac{\frac{1}{\sqrt{2\pi}\sigma} e^{-\frac{(d-\mu)^2}{2\sigma^2}} P(\mu)}{\int_{-\infty}^{+\infty} \frac{1}{\sqrt{2\pi}\sigma} e^{-\frac{(d-\mu)^2}{2\sigma^2}} P(\mu) d\mu} \quad (3.8)$$

If we assume a uniform prior imposing the condition

$$P(\mu) = \text{constant} \quad (3.9)$$

Eq (3.8) becomes:

$$P(\mu|d, \sigma) = \frac{1}{\sqrt{2\pi}\sigma} e^{-\frac{(d-\mu)^2}{2\sigma^2}}. \quad (3.10)$$

From this equation we extract the expectation value $E(\mu) = d$ and the standard deviation $\sigma(\mu) = \sigma$. In the case a precedent experiment already provided knowledge on the possible value of $\mu = \mu_0 \pm \sigma_0$ the prior would be:

$$P(\mu|\mu_0, \sigma_0) = \frac{1}{\sqrt{2\pi}\sigma_0} e^{-\frac{(\mu-\mu_0)^2}{2\sigma_0^2}}, \quad (3.11)$$

and if we substitute it in Eq. (3.8), we obtain:

$$P(\mu|d, \mu_0, \sigma_0) = \frac{1}{\sqrt{2\pi}\sigma_1} e^{-\frac{(\mu-\mu_1)^2}{2\sigma_1^2}}, \quad (3.12)$$

where:

$$\mu_1 = E(\mu) = \frac{\frac{d}{\sigma^2} + \frac{\mu_0}{\sigma_0^2}}{\frac{1}{\sigma^2} + \frac{1}{\sigma_0^2}} \quad (3.13a)$$

$$\sigma_1^2 = Var(\mu) = (\sigma_0^{-2} + \sigma^{-2})^{-1}. \quad (3.13b)$$

We can observe that the case of uniform prior distribution corresponds to the limit case of prior gaussian distribution with big σ_0 .

As we can see from Eqs. (3.13a) and (3.13b) the more the number of measurements grows the smaller the uncertainty on the parameters becomes. In case more different set of measures $\{d_i\}$ are available, it is possible to improve the knowledge of parameters. After the first measurement of d_1 the posterior distribution is:

$$P(\theta|d_1) \propto P(d_1|\theta)P(\theta). \quad (3.14)$$

after a second measurement it becomes:

$$P(\theta|d_1, d_2) \propto P(d_2|\theta, d_1)P(d_1|\theta) = P(d_1, d_2|\theta)P(\theta). \quad (3.15)$$

From this result we can see that the sequential inference gives the same result than a single inference which uses all the known information.

Therefore if we consider the $\{d_i\}$ organized in a measurement vector \mathbf{d} it is possible to generalize as:

$$P(\theta|\mathbf{d}) \propto P(\mathbf{d}|\theta)P(\theta). \quad (3.16)$$

If the d_i are independent the combined likelihood is the product of every likelihood:

$$P(\theta|\mathbf{d}) = \prod_i P(d_i|\theta)P(\theta). \quad (3.17)$$

Chapter 4

Measurement of the CKM parameters γ and $-2\beta_s$ using $B \rightarrow h^+h^-$ decays

The angle γ presented in Eq. (2.18) is the only angle of the UT that can be measured using decays governed by tree-level diagrams only, hence in a way that is free from possible contributions of physics beyond the SM [5]. However, over the years, strategies have been proposed to determine γ using loop-mediated two body B decays also called $B \rightarrow h^+h^-$ [6, 7, 8]. The relevant contribution of penguin topologies to the decay amplitudes of these decays can be seen as a great opportunity to probe the presence of physics beyond the SM. In fact, within the loops, thanks to the Heisenberg's uncertainty principle, it is possible to violate the conservation of energy. Hence very heavy particles, with masses beyond the reach of modern particle accelerators, may appear in the loops as virtual contributions. Their presence can thus modify the values of the observables of the decay, causing a disagreement between γ determined from tree-level decays and γ determined from $B \rightarrow h^+h^-$ decays.

Unfortunately, the presence of penguin diagrams introduces additional parameters in the model (so-called hadronic parameters) that can not be calculated from theory. The consequence is that these parameters must be included as unknown terms in the analysis. The effect is that the number of unknown might become larger than the number of experimental measurements available to constrain them. The strategies proposed in Refs. [6, 7, 8], make use of isospin and U-spin symmetries to reduce the number of unknown and determine the relevant parameters with better precision. The isospin symmetry is the invariance of strong interaction under the exchange of a d quark with a u quark and vice versa; the U-spin symmetry is, instead, the invariance of strong interaction under the exchange of d quark with s quark and vice versa.

Another important parameter of the CKM matrix that can be determined by studying charmless two-body B -meson decays is the mixing phase $-2\beta_s$ of the B_s^0 meson defined as:

$$\beta_s = \arg\left(-\frac{V_{ts}V_{tb}^*}{V_{cs}V_{cb}^*}\right). \quad (4.1)$$

The value of this parameter can be determined very precisely both from theory and from decays dominated by tree-level diagrams [4, 9]. Hence it is also a very valid tool to test the SM. According to Refs. [6, 7, 8] $-2\beta_s$ can also be determined from the study of $B \rightarrow h^+h'^-$.

In this thesis we will repeat the analysis performed by the LHCb collaboration in Ref. [8], but updating all the input quantities to the latest results available. The analysis consists of two approaches that will be referred as Analysis A and Analysis B. Analysis A provides a method to determine γ , leaving it as unknown parameter and constraining $-2\beta_s$ to its current theoretical determination [4]. Analysis B, on the other hand, makes use of the value of γ determined using tree-level decays to constraint it and leaves $-2\beta_s$ as an unknown parameter. In both cases the dependency of the result from the assumption of the validity of U-spin symmetry will be investigated.

Initially, only the information provided by the $B^0 \rightarrow \pi^+\pi^-$ and $B_s^0 \rightarrow K^+K^-$ decays will be used as proposed originally in Ref. [6]. Then, the extension of the analysis, suggested in Ref. [7] will be implemented including information also from $B^0 \rightarrow \pi^0\pi^0$ and $B^+ \rightarrow \pi^+\pi^0$ decays.

This chapter is structured in the following way: in the first part we will define the parameterisation of the decay amplitudes of the $B \rightarrow h^+h'^-$ decays. Then we will use the bayesian inference presented in previous Section to implement Analysis A and Analysis B.

4.1 Decay amplitudes

According to Refs. [7, 8], the decay amplitudes A_f entering the CP-violation parameter $\lambda_f = \frac{q}{p} \frac{\bar{A}_f}{A_f}$ can be written, for the considered decay modes, as:

$$\bar{A}_{\pi^+\pi^-} = D(e^{-i\gamma} - de^{i\theta}), \quad (4.2a)$$

$$\bar{A}_{\pi^0\pi^0} = \frac{1}{\sqrt{2}}D(qe^{i\theta_q}e^{-i\gamma}), \quad (4.2b)$$

$$\bar{A}_{\pi^-\pi^0} = \frac{1}{\sqrt{2}}D(1 + qe^{i\theta_q})e^{-i\gamma}, \quad (4.2c)$$

$$\bar{A}_{K^+K^-} = D' \frac{\lambda}{1 - \frac{\lambda^2}{2}} \left(e^{-i\gamma} - \frac{1 - \lambda^2}{\lambda^2} d' e^{i\theta'} \right), \quad (4.2d)$$

where γ is the CKM phase, and D , d , d' , q , θ , θ' and θ_q are unknown hadronic parameters, and $\lambda = \sin \theta_C$. Analogously the CP-conjugated amplitudes \bar{A}_f are:

$$A_{\pi^+\pi^-} = D(e^{i\gamma} - de^{i\theta}), \quad (4.3a)$$

$$A_{\pi^0\pi^0} = \frac{1}{\sqrt{2}}D(qe^{i\theta_q}e^{i\gamma}), \quad (4.3b)$$

$$A_{\pi^-\pi^0} = \frac{1}{\sqrt{2}}D(1 + qe^{i\theta_q})e^{i\gamma}, \quad (4.3c)$$

$$A_{K^+K^-} = D' \frac{\lambda}{1 - \frac{\lambda^2}{2}} \left(e^{i\gamma} - \frac{1 - \lambda^2}{\lambda^2} d' e^{i\theta'} \right). \quad (4.3d)$$

The term $\frac{q}{p}$, entering the definition of λ_f , is approximately equal to $\frac{q}{p} \simeq e^{-i\phi_D}$ for the B^0 meson and $\frac{q}{p} \simeq e^{-i\phi_s}$ for the B_s meson, where $\phi_D = 2\beta$ and $\phi_s = -2\beta_s$ are the corresponding mixing phases. This is valid under the assumption that $|\frac{q}{p}| \simeq 1$ as done in Sec. 2.2.2 for Eqs. (2.23). Using the definitions of Eqs. (2.18), (2.23), (4.2) and (4.3) it is possible to write the CP-asymmetries of the various decays in terms of the unknown parameters entering the amplitudes. The computation leads to:

$$C_{\pi^+\pi^-} = -\frac{2d \sin \theta \sin \gamma}{1 - 2d \cos \theta \cos \gamma + d^2}, \quad (4.4a)$$

$$S_{\pi^+\pi^-} = -\frac{\sin(2\beta + 2\gamma) \sim 2d \cos(\theta) \sin(2\beta + \gamma) + d^2 \sin(2\beta)}{1 - 2d \cos \theta \cos \gamma + d^2}, \quad (4.4b)$$

$$C_{\pi^0\pi^0} = -\frac{2dq \sin(\theta_q - \theta) \sin(\gamma)}{q^2 + 2dq \cos(\theta_q - \theta) \cos(\gamma) + d^2}, \quad (4.4c)$$

$$A_{\pi^+\pi^0} = 0, \quad (4.4d)$$

$$C_{K^+K^-} = \frac{2\tilde{d}' \sin(\theta') \sin(\gamma)}{1 + 2\tilde{d}' \cos(\theta') \cos(\gamma) + \tilde{d}'^2}, \quad (4.4e)$$

$$S_{K^+K^-} = -\frac{\cos(-2\beta_s + 2\gamma) + 2\tilde{d}' \cos(\theta') \sin(-2\beta_s + \gamma) + \tilde{d}'^2 \sin(-2\beta_s)}{1 + 2\tilde{d}' \cos(\theta') \cos(\gamma) + \tilde{d}'^2}, \quad (4.4f)$$

where $\tilde{d}' = d' \frac{1-\lambda^2}{\lambda^2}$ and $\lambda = \sin \theta_C$.

The CP-averaged branching fractions are defined, in terms of decay amplitudes, as:

$$B_f = \frac{1}{2} F(B_{(s)}^0 \rightarrow f) (|\bar{A}_f|^2 + |A_f|^2), \quad (4.5)$$

where

$$F(B^0 \rightarrow \pi^+\pi^-) = \frac{\sqrt{m_{B^0}^2 - 4m_{\pi^+}^2}}{m_{B^0}^2} \tau_{B^0}, \quad (4.6a)$$

$$F(B^0 \rightarrow \pi^0\pi^0) = \frac{\sqrt{m_{B^0}^2 - 4m_{\pi^0}^2}}{m_{B^0}^2} \tau_{B^0}, \quad (4.6b)$$

$$F(B_s^0 \rightarrow K^+K^-) = \frac{\sqrt{m_{B_s^0}^2 - 4m_{K^+}^2}}{m_{B_s^0}^2} [2\tau_{B_s^0} - (1 - y_s^2)\tau(B_s^0 \rightarrow K^+K^-)], \quad (4.6c)$$

with τ_{B^0} and $\tau_{B_s^0}$ the average lifetimes of B^0 and B_s^0 mesons, respectively, $\tau(B_s^0 \rightarrow K^+K^-)$ is the effective lifetime measured using $B_s^0 \rightarrow K^+K^-$ decays and $y_s = \frac{\Delta\Gamma_s}{2\Gamma_s}$. Including the definitions of the amplitudes of Eqs. (4.2) and (4.3) we obtain:

$$B_{\pi^+\pi^-} = F(B^0 \rightarrow \pi^+\pi^-) |D|^2 (1 - 2d \cos(\theta) \cos(\gamma) + d^2), \quad (4.7a)$$

$$B_{\pi^0\pi^0} = F(B^0 \rightarrow \pi^0\pi^0) \frac{|D|^2}{2} (q^2 + 2dq \cos(\theta_q - \theta) \cos(\gamma) + d^2), \quad (4.7b)$$

$$B_{\pi^+\pi^0} = F(B^+ \rightarrow \pi^+\pi^0) \frac{|D|^2}{2} (1 + q^2 + 2q \cos(\theta_q), \quad (4.7c)$$

$$B_{K^+K^-} = F(B_s^0 \rightarrow K^+K^-) \frac{\lambda^2}{(1 - \frac{\lambda^2}{2})^2} |D'|^2 (1 + 2\tilde{d}' \cos(\theta') \cos(\gamma) + \tilde{d}'^2). \quad (4.7d)$$

All the physics inputs used to implement the above-defined constraints are reported in Tab. 4.1.

Table 4.1: Physics inputs used in the analyses described in this Section.

Quantity	Value	Reference
$C_{\pi^+\pi^-}$	-0.34 ± 0.06	[10]
$S_{\pi^+\pi^-}$	-0.63 ± 0.05	[10]
$\rho(C_{\pi^+\pi^-}, S_{\pi^+\pi^-})$	0.45	[10]
$C_{\pi^0\pi^0}$	-0.33 ± 0.22	[12]
$C_{K^+K^-}$	0.20 ± 0.06	[10]
$S_{K^+K^-}$	0.18 ± 0.06	[10]
$\rho(C_{K^+K^-}, S_{K^+K^-})$	0.01	[10]
$B_{\pi^+\pi^-} \times 10^6$	5.10 ± 0.19	[12]
$B_{\pi^+\pi^0} \times 10^6$	5.48 ± 0.35	[12]
$B_{\pi^0\pi^0} \times 10^6$	1.59 ± 0.18	[12]
$B_{K^+K^-} \times 10^6$	24.8 ± 1.7	[12]
$\sin 2\beta$	0.689 ± 0.018	[4]
λ	0.22574 ± 0.00089	[4]
m_{B^0} [MeV/c ²]	5279.63 ± 0.15	[3]
m_{B^+} [MeV/c ²]	5279.32 ± 0.14	[3]
$m_{B_s^0}$ [MeV/c ²]	5366.89 ± 0.19	[3]
m_{π^+} [MeV/c ²]	139.57061 ± 0.00024	[3]
m_{π^0} [MeV/c ²]	134.9770 ± 0.0005	[3]
m_{K^+} [MeV/c ²]	493.677 ± 0.016	[3]
τ_{B^0} [ps]	1.520 ± 0.004	[12]
τ_{B^+} [ps]	1.638 ± 0.004	[12]
$\tau_{B_s^0}$ [ps]	1.509 ± 0.004	[12]
$\Delta\Gamma_s/\Gamma_s$	0.132 ± 0.008	[12]
$\tau(B_s^0 \rightarrow K^+K^-)$ [ps]	1.407 ± 0.017	[11]

4.2 Determination of γ and $-2\beta_s$ from $B^0 \rightarrow \pi^+\pi^-$ and $B_s^0 \rightarrow K^+K^-$ decays

The method implemented here was proposed by Fleischer in Ref. [6], using the $B^0 \rightarrow \pi^+\pi^-$ and $B_s^0 \rightarrow K^+K^-$ decays. The method assumes the validity of U-spin symmetry in order to reduce the number of unknown. In fact, we have only 6 constraints represented by C_f , S_f and B_f for the two decays, and the 9 unknown γ , 2β , $-2\beta_s$, d , θ , D , d' , θ' and D' . The value of 2β is well known from independent measurements and can hence be constrained, reducing the number of unknown to 8. Assuming the validity of U-spin the following relations hold

$$d = d', \quad (4.8a)$$

$$\theta = \theta', \quad (4.8b)$$

$$|D| = |D'|, \quad (4.8c)$$

$$(4.8d)$$

further reducing the number of unknown to 5. However U-spin symmetry is known to be broken and the effect must be parameterised. Some of the effects of this breaking can be computed theoretically, while others must be considered as unknown parameters. According to Ref. [8] $|D'|$, d' and θ' can be written as:

$$|D'| = \left| \frac{D'}{D} \right|_{fact} |D| |1 + r_D e^{i\theta_{rD}}|, \quad (4.9a)$$

$$d' e^{i\theta'} = d e^{i\theta} \frac{1 + r_G e^{i\theta_{rG}}}{1 + r_D e^{i\theta_{rD}}}, \quad (4.9b)$$

where:

$$\left| \frac{D'}{D} \right|_{fact} = 1.41^{+0.20}_{-0.11}. \quad (4.10)$$

is the term that can be determined theoretically [17]. Given the asymmetric error of this parameter an asymmetric Gaussian prior is used for it. The parameters r_D and r_G are the relative magnitudes introduced by the breaking, while θ_{rD} and θ_{rG} are the corresponding phase shifts. In the following we will make no assumption on θ_{rD} and θ_{rG} using priors between $[-180, 180]$. Concerning the magnitudes r_D and r_G they will be let free to vary between 0 and κ . In this way the parameter κ plays the role of the maximum magnitude of U-spin breaking effects that are allowed in the analysis. Different values of κ will be tested, between 0 and 1, corresponding to allowing 0% and 100% breaking of the symmetry, respectively. To mitigate the introduction of these further unknown, as explained previously, γ and $-2\beta_s$ are alternatively constrained using the current knowledge of their values from independent measurements.

Table 4.2: Priors used in Analysis A and Analysis B. In the case the priors are expressed in terms of ranges, flat priors are used. In case the prior is expressed in terms of a central value and an error then Gaussian priors are used.

Quantity	Priors	
	Analysis A	Analysis B
d	$[0, 20]$	$[0, 20]$
θ	$[-180^\circ, +180^\circ]$	$[-180^\circ, +180^\circ]$
θ_q	$[-180^\circ, +180^\circ]$	$[-180^\circ, +180^\circ]$
γ	$[-180^\circ, +180^\circ]$	$(70.0 \pm 4.2)^\circ$
$-2\beta_s$	—	$[-180^\circ, +180^\circ]$

4.2.1 Analysis A

In the SM the value of $-2\beta_s$ given by an approximation of order λ^4 is given by:

$$-2\beta_s = 2\lambda^2 \bar{\eta} [1 + \lambda^2 (1 - \bar{\rho})], \quad (4.11)$$

where $\bar{\rho}$ and $\bar{\eta}$ can be written as functions of β and γ as:

$$\bar{\rho} = \frac{\sin \beta \cos \gamma}{\sin(\beta + \gamma)}, \quad (4.12a)$$

$$\bar{\eta} = \frac{\sin \beta \sin \gamma}{\sin \beta + \gamma}, \quad (4.12b)$$

hence $-2\beta_s$ is expressed in these terms in order to eliminate one unknown.

Flat priors, with the ranges shown in Table 4.2, are used for θ , d and γ , while for all the physics inputs Gaussian constraints are used. No prior is defined for the unknown $|D|$. As it can be seen, inverting Eq. (4.7a) it is possible to avoid to extract this parameter using a flat prior. We decided instead to extract $B_{\pi^+\pi^-}$ using a Gaussian prior and then use this information to compute the value of $|D|$. In this way significant CPU power is gained without affecting at all the validity of the analysis.

The analysis has been performed assuming different values of the U-spin breaking parameter κ , with particular attention to the change in the posterior distribution of γ as a function of κ . The dependencies of the 68% and 95% probability intervals for γ are reported in Fig. 4.1. The plot shows a relevant dependency of the width of

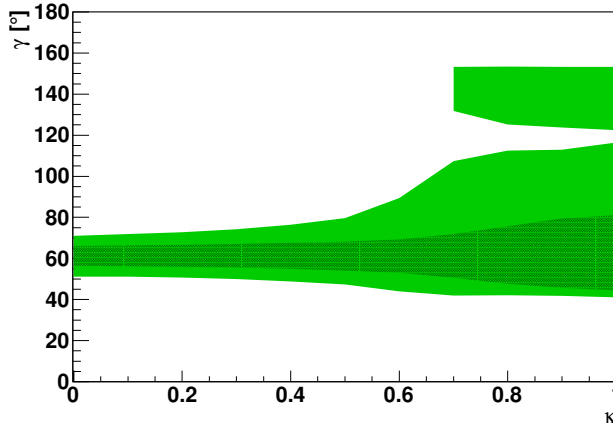


Figure 4.1: Dependency of the (dark green) 68% and (bright green) 95% probability intervals for γ as a function of the U-spin breaking parameter κ . The intervals are obtained from Analysis A using only the constraints from $B^0 \rightarrow \pi^+\pi^-$ and $B_s^0 \rightarrow K^+K^-$ decays.

the probability intervals as a function of κ . In particular for $\kappa > 0.6$ a small second solution appears. This is mainly driven by the non-linearity of the constraints in Eqs. (4.4) and (4.7). Since typical U-spin breaking effects are expected to be around 30% [15, 16], we decide to quote, in a conservative way, the result obtained using $\kappa = 0.5$. The corresponding probability intervals are reported in Table 4.3, while the corresponding posterior distributions are shown in Fig. 4.2.

4.2.2 Analysis B

In this alternative approach, instead, $-2\beta_s$ is left as a free parameter with a flat prior in the range $[-180, 180]^\circ$. A Gaussian prior is used for the angle γ corresponding

Table 4.3: Probability intervals for the unknown parameters determined from Analysis A. Only the constraints from the $B^0 \rightarrow \pi^+\pi^-$ and $B_s^0 \rightarrow K^+K^-$ decays are used.

Quantity	68% prob.	95% prob.
$ D $ [$MeV^{\frac{1}{2}}ps^{\frac{1}{2}}$]	[0.103, 0.117]	[0.095, 0.125]
d	[0.30, 0.52]	[0.24, 0.75]
θ	[124°, 152°]	[103°, 161°]
$ D' $ [$MeV^{\frac{1}{2}}ps^{\frac{1}{2}}$]	[0.127, 0.193]	[0.096, 0.232]
d'	[0.33, 0.50]	[0.28, 0.65]
θ'	[119°, 144°]	[104°, 157°]
γ	[54°, 68°]	[47°, 80°]

Table 4.4: Probability intervals for the unknown parameters determined from Analysis B. Only the constraints from the $B^0 \rightarrow \pi^+\pi^-$ and $B_s^0 \rightarrow K^+K^-$ decays are used.

Quantity	68% prob.	95% prob.
$ D $ [$MeV^{\frac{1}{2}}ps^{\frac{1}{2}}$]	[0.101, 0.111]	[0.096, 0.116]
d	[0.41, 0.60]	[0.33, 0.74]
θ	[139°, 152°]	[130°, 159°]
$ D' $ [$MeV^{\frac{1}{2}}ps^{\frac{1}{2}}$]	[0.119, 0.186]	[0.089, 0.228]
d'	[0.34, 0.52]	[0.28, 0.69]
θ'	[123°, 151°]	[106°, 163°]
$-2\beta_s$	[−6.7°, 3.6°]	[−11.9°, 8.9°]

to its determination from tree-level decays $\gamma = (70.0 \pm 4.2)^\circ$ [4]. The probability intervals for $-2\beta_s$ as a function of the U-spin breaking parameter κ are shown in Fig. 4.3. In this case the dependency on κ is less pronounced with respect to γ . The probability intervals obtained for $\kappa = 0.5$ are reported in Table 4.4, and the corresponding posterior distributions are shown in Fig. 4.4.

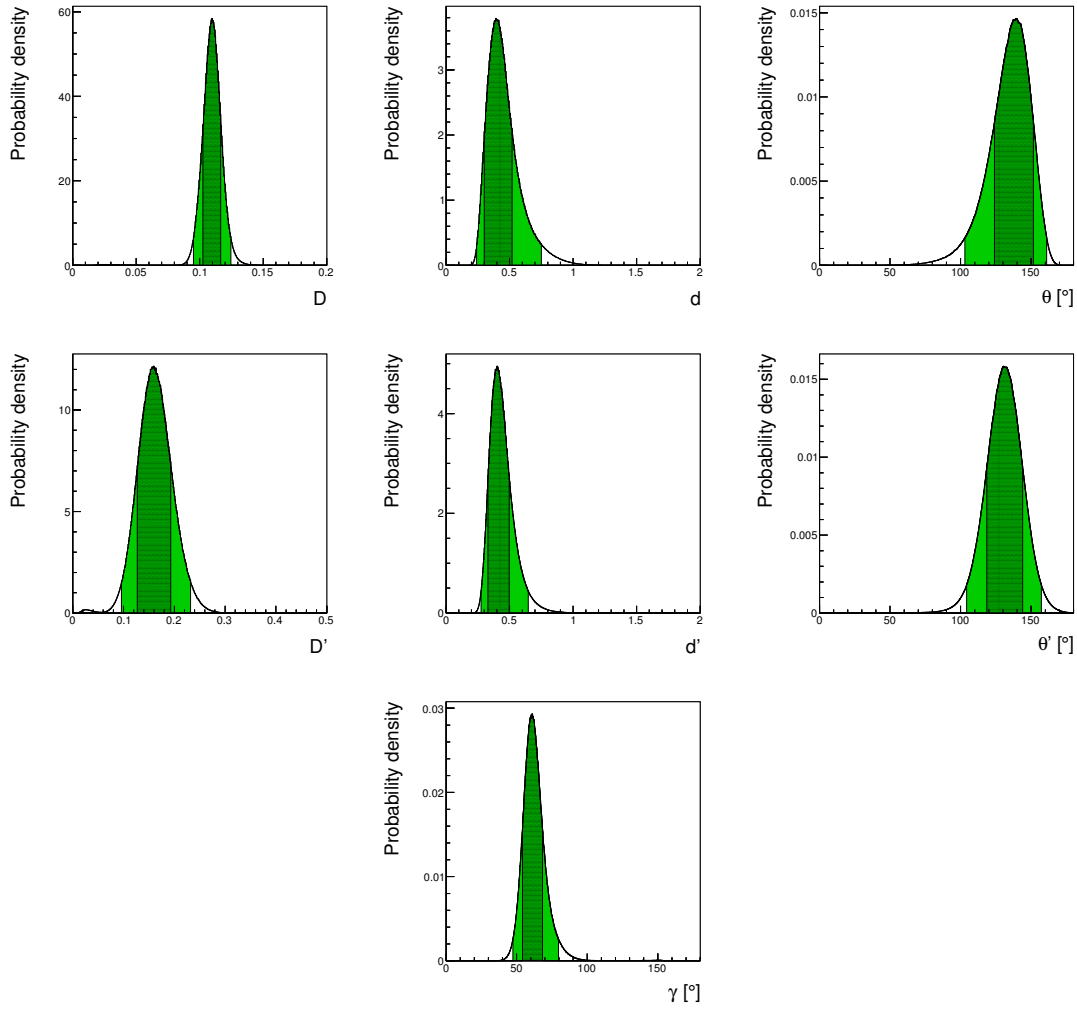


Figure 4.2: Posterior probability distributions for (top left) $|D|$, (top centre) d , (top right) θ , (middle left) $|D'|$, (middle centre) d' , (middle right) θ' and (bottom) γ , obtained from Analysis A and using only the inputs from $B^0 \rightarrow \pi^+\pi^-$ and $B_s^0 \rightarrow K^+K^-$ decays. The intervals corresponding to (dark green) 68% and (bright green) 95% probability are also shown.

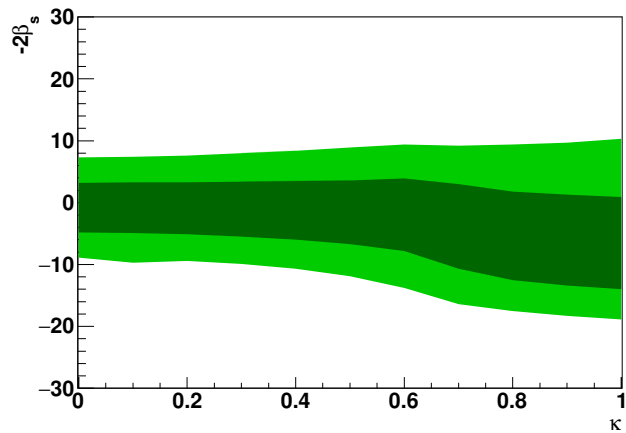


Figure 4.3: Dependency of the (dark green) 68% and (bright green) 95% probability intervals for $-2\beta_s$ as a function of the U-spin breaking parameter κ . The intervals are obtained from Analysis B using only the constraints from $B^0 \rightarrow \pi^+\pi^-$ and $B_s^0 \rightarrow K^+K^-$ decays.

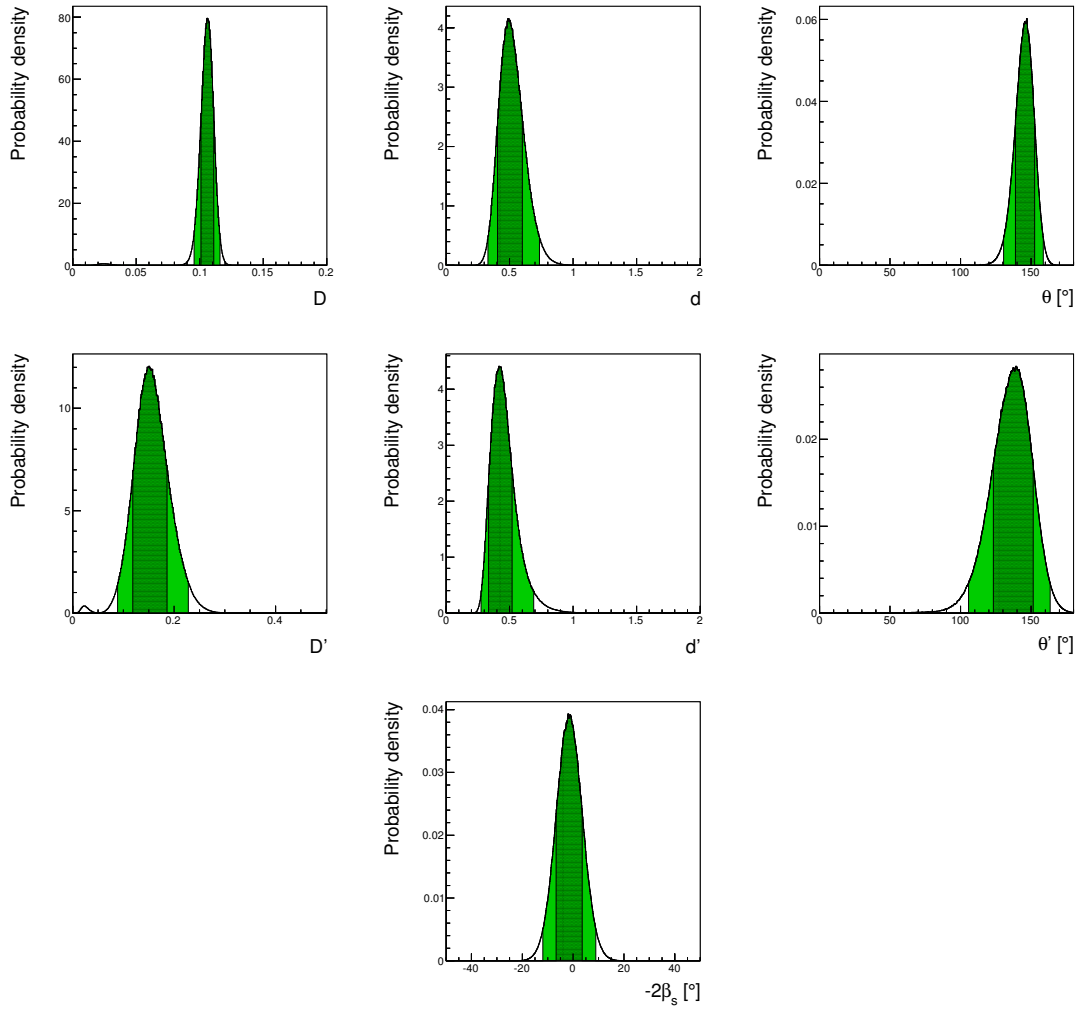


Figure 4.4: Posterior probability distributions for (top left) $|D|$, (top centre) d , (top right) θ , (middle left) $|D'|$, (middle centre) d' , (middle right) θ' and (bottom) $-2\beta_s$, obtained from Analysis B and using only the inputs from $B^0 \rightarrow \pi^+\pi^-$ and $B_s^0 \rightarrow K^+K^-$ decays. The intervals corresponding to (dark green) 68% and (bright green) 95% probability are also shown.

4.3 Inclusion of $B^0 \rightarrow \pi^0\pi^0$ and $B^+ \rightarrow \pi^+\pi^0$

In order to further mitigate the effects due to the breaking of U-spin symmetry it is possible to use the isospin relation that connects the $B^0 \rightarrow \pi^+\pi^-$, the $B^0 \rightarrow \pi^0\pi^0$ and the $B^0 \rightarrow \pi^+\pi^0$ decays. Since the isospin symmetry is known to be almost perfect the assumption of its validity introduce no additional uncertainty to the analysis. In Refs.[13, 14] studies have been performed to determine the uncertainty related to possible isospin breaking finding it small for the purpose of our analysis. The two new decays introduce 3 additional constraints ($C_{\pi^0\pi^0}$, $B_{\pi^0\pi^0}$ and $B_{\pi^+\pi^0}$) in exchange of only two additional unknown (q and θ_q).

The analysis is performed in the same way as in Sec. 4.2. In order reduce the usage of computing power a further optimisation is implemented. The constraint in Eq. (4.7c) is substituted with a linear combination of Eqs. (4.7b) and (4.7c). In such a way, the branching fractions of the $B^0 \rightarrow \pi^0\pi^0$ and $B^+ \rightarrow \pi^+\pi^0$ decays are extracted according to their Gaussian priors, and are used to calculate the corresponding value for q .

4.3.1 Analysis A

The probability intervals for γ as a function of κ are studied and shown in Fig. 4.5. With respect to Fig. 4.1 it is evident that the effect of U-spin breaking is mitigated

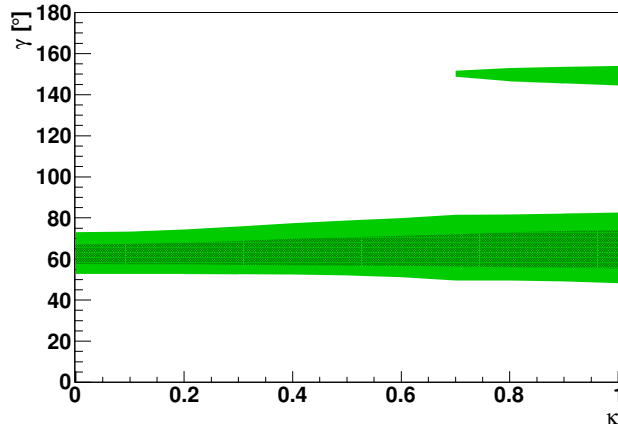


Figure 4.5: Dependency of the (dark green) 68% and (bright green) 95% probability intervals for γ as a function of the U-spin breaking parameter κ . The intervals are obtained from Analysis A using all the constraints provided by the $B \rightarrow h^+h'^-$ decays.

by the inclusion of the additional constraints. The probability intervals, assuming $\kappa = 0.5$ are reported in Tab. 4.5, while the corresponding posterior distributions are shown in Fig. 4.6.

4.3.2 Analysis B

The probability intervals for γ as a function of κ are studied and shown in Fig. 4.7. With respect to Fig. 4.1 the effect of additional constraints is less evident

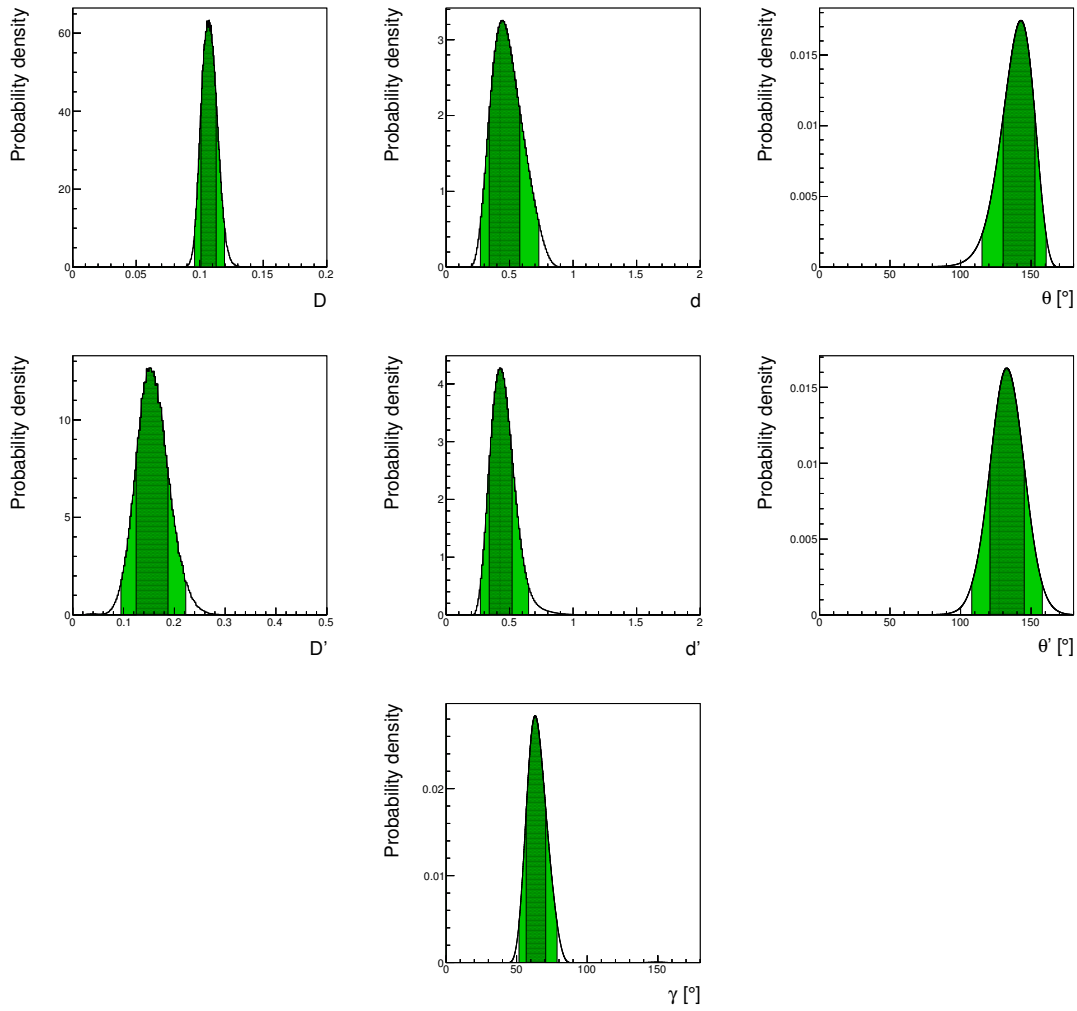


Figure 4.6: Posterior probability distributions for (top left) $|D|$, (top centre) d , (top right) θ , (middle left) $|D'|$, (middle centre) d' , (middle right) θ' and (bottom) γ , obtained from Analysis A and all the constraints provided by $B \rightarrow h^+h'^-$ decays. The intervals corresponding to (dark green) 68% and (bright green) 95% probability are also shown.

but anyhow not negligible. The probability intervals, assuming $\kappa = 0.5$ are reported in Tab. 4.6, while the corresponding posterior distributions are shown in Fig. 4.6.

Table 4.5: Probability intervals for the unknown parameters determined from Analysis A. All the constraints from all the $B \rightarrow h^+h'^-$ decays are used.

Quantity	68% prob.	95% prob.
$ D $ [$MeV^{\frac{1}{2}}ps^{\frac{1}{2}}$]	[0.101, 0.113]	[0.096, 0.120]
d	[0.35, 0.58]	[0.28, 0.72]
θ	[130°, 153°]	[115°, 160°]
$ D' $ [$MeV^{\frac{1}{2}}ps^{\frac{1}{2}}$]	[0.125, 0.188]	[0.095, 0.223]
d'	[0.34, 0.51]	[0.29, 0.66]
θ'	[121°, 145°]	[108°, 158°]
γ	[57°, 71°]	[52°, 79°]

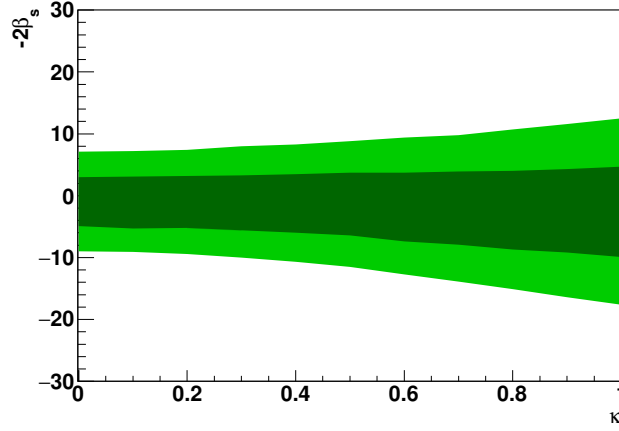


Figure 4.7: Dependency of the (dark green) 68% and (bright green) 95% probability intervals for $-2\beta_s$ as a function of the U-spin breaking parameter κ . The intervals are obtained from Analysis B using all the constraints provided by the $B \rightarrow h^+h'^-$ decays.

Table 4.6: Probability intervals for the unknown parameters determined from Analysis B. All the constraints from all the $B \rightarrow h^+h'^-$ decays are used.

Quantity	68% prob.	95% prob.
$ D $ [$MeV^{\frac{1}{2}}ps^{\frac{1}{2}}$]	[0.101, 0.110]	[0.096, 0.115]
d	[0.44, 0.63]	[0.36, 0.72]
θ	[140°, 153°]	[132°, 158°]
$ D' $ [$MeV^{\frac{1}{2}}ps^{\frac{1}{2}}$]	[0.118, 0.183]	[0.090, 0.223]
d'	[0.35, 0.53]	[0.28, 0.68]
θ'	[123°, 151°]	[107°, 163°]
$-2\beta_s$	[-6.4°, 3.7°]	[-11.5°, 8.8°]

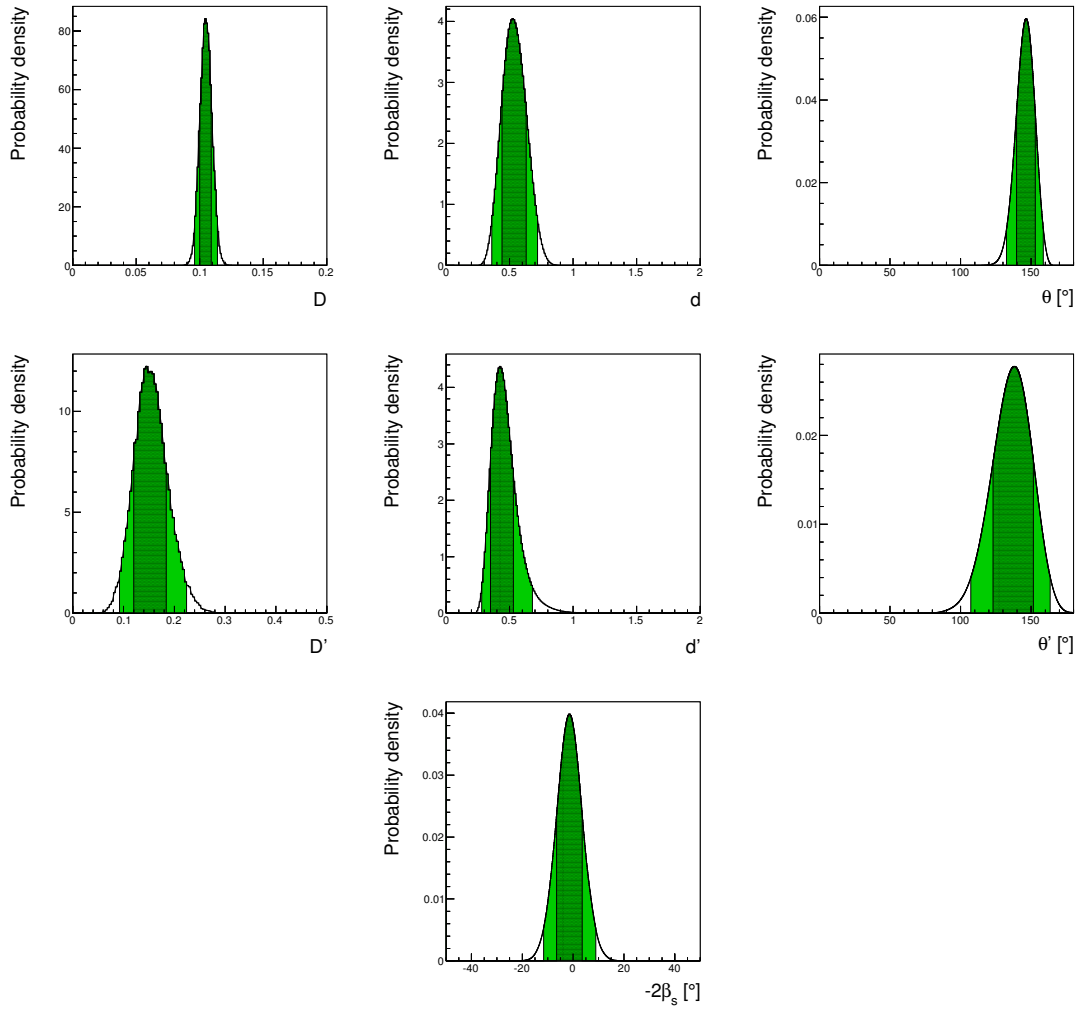


Figure 4.8: Posterior probability distributions for (top left) $|D|$, (top centre) d , (top right) θ , (middle left) $|D'|$, (middle centre) d' , (middle right) θ' and (bottom) $-2\beta_s$, obtained from Analysis B and all the constraints provided by $B \rightarrow h^+h'^-$ decays. The intervals corresponding to (dark green) 68% and (bright green) 95% probability are also shown.

Chapter 5

Conclusions

Using CP asymmetries and branching fractions of charmless two-body decays of beauty mesons we have determined the angle γ and the B_s^0 mixing phase $-2\beta_s$, that are fundamental parameters of the CKM matrix. A bayesian inference approach has been used to extract these parameters from the measurements. In section 4.2.1 and 4.2.2, we have determined γ and $-2\beta_s$, respectively, using the constraints provided by the $B^0 \rightarrow \pi^+\pi^-$ and $B_s^0 \rightarrow K^+K^-$ decays. In sections 4.3.1 and 4.3.2 we performed the same analyses including also constraints from $B^0 \rightarrow \pi^0\pi^0$ and $B^+ \rightarrow \pi^+\pi^0$ decays. For each analysis we also studied the effects of allowing the breaking of the U-spin symmetry, that is the main theoretical systematic affecting the analysis. The determination of γ results to be slightly affected by U-spin breaking up to more than a 60% breaking. After this threshold the probability intervals for γ are much enlarged and even a second solution appears. This effect is much reduced when including the constraints from $B^0 \rightarrow \pi^0\pi^0$ and $B^+ \rightarrow \pi^+\pi^0$. On the contrary the probability interval for β_s is only marginally affected by the breaking of the U-spin symmetry and the inclusion of the constraints from $B^0 \rightarrow \pi^0\pi^0$ and $B^+ \rightarrow \pi^+\pi^0$ decays has a small effect. Anyhow, within the theory community there is general consensous that U-spin breaking effects are expected to be around 30%. Hence we decided to conservatively quote as final results, those obtained allowing up to 50% of U-spin breaking effects. Considering the posterior distributions obtained from the bayesian analysis we obtain for γ and $-2\beta_s$

$$\gamma = (63.7 \pm 6.8)^\circ, \quad (5.1)$$

$$-2\beta_s = (-1.5 \pm 5)^\circ. \quad (5.2)$$

The results are in very good agreement with the current standard model determination of these parameters that are $\gamma = (70.0 \pm 4.2)^\circ$ and $-2\beta_s = (-1.2 \pm 1.8)^\circ$ [4].

Bibliography

- [1] N. Cabibbo, *Unitary symmetry and leptonic decays*, Phys. Rev. Lett. **10** (1963) 531;
- [2] M. Kobayashi and T. Maskawa, *CP violation in the renormalizable theory of weak interaction*, Prog. Theor. Phys. **49** (1973) 652;
- [3] M. Tanabashi et al. (Particle Data Group), *Review of particle physics*, Phys. Rev. **D98** (2018) 010001.
- [4] M. Bona et al. (UTfit collaboration), *The unitarity triangle fit in the standard model and hadronic parameters from lattice QCD: A reappraisal after the measurements of Δm_s and $\mathcal{BR}(B \rightarrow \tau \nu_\tau)$* , JHEP **10** (2006) 081, arXiv:hep-ph/0606167, updated results and plots available at <http://www.utfit.org/>.
- [5] J. Brod and J. Zupan, *The ultimate theoretical error on γ from $B \rightarrow DK$ decays*, JHEP **01** (2014) 051, arXiv:1308.5663; J. Brod, *Electroweak effects in the extraction of the CKM angle γ from $B \rightarrow DK$ decays*, Phys. Lett. **B743** (2015) 56, arXiv:1412.3173.
- [6] R. Fleischer, *New strategies to extract β and γ from $B_d \rightarrow \pi^+ \pi^-$ and $B_s \rightarrow K^+ K^-$* , Phys. Lett. **B459** (1999) 306, arXiv:hep-ph/9903456.
- [7] M. Ciuchini et al., *Testing the standard model and searching for new physics with $B^0 \rightarrow \pi^+ \pi^-$ and $B_s^0 \rightarrow K^+ K^-$ decays*, JHEP **10** (2012) 29, arXiv:1205.4948.
- [8] R. Aaij et al. (LHCb collaboration), *Determination of γ and $-2\beta_s$ from charmless two-body decays of beauty mesons*, Phys. Lett. **B739** (2015) 1, arXiv:1408.4368.
- [9] R. Aaij et al. (LHCb collaboration), *Precision measurement of CP violation in $B_s^0 \rightarrow J/\psi K^+ K^-$ decays*, Phys. Rev. Lett. **114** (2015) 041801, arXiv:1411.3104.
- [10] R. Aaij et al. (LHCb collaboration), *Measurement of CP asymmetries in two-body $B_{(s)}^0$ -meson decays to charged pions and kaons*, Phys. Rev. **D98** (2018) 032004.
- [11] R. Aaij et al. (LHCb collaboration), *Effective lifetime measurements in the $B_s^0 \rightarrow K^+ K^-$, $B^0 \rightarrow K^+ \pi^-$ and $B_s^0 \rightarrow \pi^+ K^-$ decays*, Phys. Lett. **B736** (2014) 446.

- [12] Y. Amhis et al. (Heavy Flavor Averaging Group), *Averages of b -hadron, c -hadron, and τ -lepton properties as of summer 2016*, Eur. Phys. J. **C77** (2017) 895, arXiv:1612.07233, updated results and plots available at <http://www.slac.stanford.edu/xorg/hflav/>.
- [13] M. Bona et al. (UTFit collaboration), *Improved determination of the CKM angle α from $B \rightarrow \pi\pi$ decays*, Phys. Rev. **D76** (2007) 014015, arXiv:hep-ph/0701204.
- [14] J. Charles et al., *Isospin analysis of charmless B -meson decays*, Eur. Phys. J. **C77** (2017) 574, arXiv:1705.02981.
- [15] M. Gronau, *U-spin breaking in CP asymmetries in B decays*, Phys. Lett. **B727** (2013) 136, arXiv:1308.3448.
- [16] M. Nagashima et al., *U-spin tests of the standard model and new physics*, Mod. Phys. Lett. **A23** (2008) 1175, arXiv:hep-ph/0701199.
- [17] G. Duplancic et al., *$B, B_s \rightarrow K$ form factors: an update of light-cone sum rule results*, Phys. Rev. **D78** (2008) 054015, arXiv:0805.4170.
- [18] L. Wolfenstein, *Parametrization of the Kobayashi-Maskawa Matrix*, Phys. Rev. Lett. **51** (1983) 1945.

Acknowledgements

For every day of these last few months I found myself wondering more and more how I got here. As a traveller looking back to his path I remembered every single joy and every moment of despair, every little win and all the losses. As I go on taking this one step of my life, I also cannot forget all the people who stood beside me, those who were there from the very beginning and those who came along the way.

Of all those who accompanied me I would like to especially thank Federica, because without her support and care I truly think I would not have been able to arrive this far. I also have to spend some words for my family: not only they managed to get through all this time in spite of my many peculiarities, they were so good that in every important moment of my life they have succeeded in being there to give me a hand or, mostly, to do something out of the way in order to show the world their affection for me. I would like to especially thank my father, who has always stood by my side no matter what, and my mother, who has always seen the better part of me, even when it was not there.

I would like to thank Stefano for helping me out in my first experience in this new world, and for doing it with such kindness as he did. I also wanted to thank my friends, for not having thrown anything at me when I was talking about “foolish physicist’s stuff” and instead for always being there to comfort me when I needed it the most. In the end I would like to express my gratitude to all those who spent a kind word or a nice thought for me: they all gave me more than I could have asked for. I sincerely hope never to betray those who entrusted me with their care and their love.